On secondary instability of a transitional separation bubble

Declarations of interest: none

On secondary instability of a transitional separation bubble

Zhiyin Yang [a, *] and Ibrahim E. Abdalla [b]

[a]*School of Mechanical Engineering and the Built Environment, College of Engineering and Technology, University of Derby, Derby DE22 3AW, U.K.*
[b]*Department of Mechanical Engineering, Jubail University College, Al Jubail 35716, Saudi Arabia*

Abstract

It is well established in the natural transition of an attached boundary layer that the transition process starts with a two–dimensional primary instability (Tollmien–Schlichting wave, denoted as TS wave), followed by usually a three-dimensional secondary instability (fundamental mode or subharmonic mode) leading to the breakdown to turbulence. However, the transition process of a separation bubble (laminar flow or laminar boundary layer at separation and transition occurs downstream of the separation, leading to turbulence at reattachment) is less well understood, especially on the nature of secondary instability.

The focus of this paper is on trying to advance our understanding of secondary instability of a transitional separation bubble on a flat plate with a blunt leading edge (separation is induced geometrically at the leading edge) under a very low free-stream turbulence level (< 0.1%). Large-Eddy Simulation (LES) is employed in the current study with a dynamic sub-grid-scale model. The numerical flow visualisation together with the spectral analysis has indicated that a three dimensional secondary instability, the elliptical instability, which occurs for fundamental frequency is the main mechanism at work whereas the subharmonic mode in the form of vortex-pairing is hardly active. There is no evidence for the existence of hyperbolic instability in the braid region either.

Keywords: Secondary Instability; Transition; Separation Bubble, Large-Eddy Simulation; Elliptical Instability.

1. Introduction

Laminar-to-turbulent transition in separated flows is a common feature and plays a very important role in aerospace aerodynamics and many other engineering flows. Boundary layer transition may be broadly classified into two main categories: attached boundary layer transition and separated boundary layer transition (for turbomachinery flows a third class called wake induced transition has been added by many researchers). Separated boundary layer transition is quite common in many practical engineering flows but the research efforts in this area is relatively less and hence our understanding is limited. By comparison extensive research has been carried out for attached boundary layer transition and the transition process is generally much better understood with a

[*] Corresponding author: Z.Yang@derby.ac.uk

classical description of the transition starting from a primary instability, followed by a secondary instability and bifurcations etc. which successively break the symmetries of the original problem (Manneville, 1990). More specifically, the transition process in an attached boundary layer can be divided into the following several stages (Schmid and Henningson, 2001).

i). Receptivity stage – how the disturbances are projected into growing eigenmodes, or how they enter or otherwise induce disturbances in a boundary layer.

ii). Primary instability – small disturbances are amplified due to a so called primary instability of the flow till they reach a size where nonlinear growth starts. This amplification can be in the form of exponential growth of eigenmodes, nonmodal growth of optimal disturbances, or nonmodal responses to forcing.

iii). Secondary instability – usually once a disturbance reaches a finite amplitude it often saturates and transforms the flow into a kind of new, periodic state at the fundamental frequency of the primary instability. Very rarely the primary instability can lead the flow directly into a turbulent state and the new periodic flow becomes a base on which a so called secondary instability can occur. The growth rate of disturbances at secondary stage is usually much larger than that of primary instability stage.

iv). Breakdown stage – nonlinearities and possibly higher instabilities excite an increasing number of scales and frequencies in the flow. This stage is more rapid than both the linear and secondary instability stages.

Transition process in separation bubbles are more complex and depends on many factors such as free-stream turbulence intensity (Simoni *et al*. 2017; Istvan and Yarusevych 2018) and passing wakes in turbomachinery flows (Sarkar 2008). Our understanding of the transition process in separation bubbles is limited apart from the primary instability stage which is due to the Kelvin-Helmholtz (KH) mechanism in the absence of any large magnitude environmental disturbances as demonstrated vigorously by the LES study of Yang and Voke (2000a, 2001) for a transitional separation bubble on a flat plate with a semi-circular leading edge and by the LES study of Abdalla and Yang (2004) on a flat plate with a blunt leading edge, and by many other experimental and numerical studies (Burgmann *et al.*, 2008; McAuliffe and Yaras, 2009, 2010; Satta *et al.*, 2010; Dahnert *et al.*, 2012). What is happening after the primary instability stage and how the three-dimensional motion develops from the initial quasi two-dimensional KH rolls via a secondary instability is not well understood.

Several studies have been carried out to investigate secondary instability of transitional separation bubbles formed on a flat plate where a laminar boundary layer develops over certain distance and separates due to an adverse pressure gradient (Rist *et al*., 1996; Maucher *et al*., 1990, 2000, Marxen *et al.*, 2003, 2013; Rodriguez and Gennaro, 2015). It was found that a mechanism of secondary, temporal amplification exists in transitional separation bubbles for large boundary layer Reynolds numbers at separation (Maucher *et al*., 1999, 2000) and this

new mechanism of secondary instability is likely to have great impact on the onset of transition. Marxen *et al.* (2003) carried out numerical and experimental studies of a transitional separation bubble due to an adverse pressure gradient on a flat plate and found out that two-dimensional disturbances were considerably more amplified than oblique waves at the forcing frequency. They concluded that the amplitude of the 3-D disturbances further upstream of the transition location is of no significant importance for the transition process, supporting the findings by Maucher *et al*. (1999, 2000) that a kind of absolute secondary instability existed after the primary instability stage which leads to three dimensionality and has a major impact on the onset of transition. Michelis *et al.* (2018) studied the three-dimensional, spatial-temporal flow development in the aft portion of a laminar separation bubble formed on a flat plate due to an adverse pressure gradient. Their studied showed that the spanwise deformations of the dominant vortical structures are caused by a superposition of normal and oblique instability modes initiating upstream of separation. Jones *et al.* (2008) studied numerically transition process of forced and unforced transitional separation bubbles on an aerofoil at incidence. They found that two secondary instabilities were active, one in elliptic regions of fluid flow (spanwise vortex core regions) and another in hyperbolic regions of fluid flow (regions between two consecutive spanwise vortices called Braid regions). They argued that those regions of pronounced disturbance growth appear to match regions of instability growth identified in mixing layers and bluff-body wakes and hence suggested that the mechanism of vortex core region instability is similar to that of elliptic instability (Kerswell, 2002) while the mechanism of braid region instability is similar to that of mode-B instability or called the hyperbolic instability (Williamson, 1996a).

In a two dimensional attached boundary layer, it is well understood that three dimensional disturbances become significantly amplified due to a secondary instability once two dimensional primary disturbances have reached sufficiently high amplitudes (Herbert, 1988) and secondary instabilities may be of fundamental or subharmonic nature, i.e., the secondary instability amplifies disturbances with fundamental or subharmonic frequency with respect to the two dimensional one. This is also well established for free shear layers that fundamental type of secondary instability is associated with the formation of streamwise vortical structures called "ribs" while subharmonic type of secondary instability is associated with the merger of neighbour spanwise vortices called "vortex pairing" (Ho and Huerre, 1984; Huang and Ho, 1990; Metcalfe *et al*., 1987; Moser and Rogers, 1993). Evidence exists for transitional separations bubbles that different types of secondary instabilities could occur for both fundamental and subharmonic frequencies (Maucher *et al*., 2000) although Jones *et al.* (2008) considered only fundamental type of secondary instabilities. McAuliffe and Yaras (2009) carried out a detailed experimental study on a transitional separation bubble and the vortex pairing phenomenon initiated by a subharmonic instability was observed. Maxren *et al.* (2013) presented detailed analysis of vortex formation and

its evolution in a forced (two-dimensional perturbation at a forcing frequency) transitional separation bubble induced by an adverse pressure gradient on a semi-infinite flat plate. They demonstrated that a combination of more than one secondary instability mechanism was active: an elliptic instability in the vortex core region leading to a spanwise deformation of the vortex core with a spanwise wavelength of the order of the size of the vortex; and another instability in the braid region which occurred for much higher spanwise wavenumbers compared to the elliptic instability, leading to a quick disintegration of the spanwise vortex into small-scale turbulence. They observed that both those secondary instability mechanisms occurred for fundamental and subharmonic frequencies with respect to the vortex shedding frequency. They argued that the instability in the braid region was a hyperbolic instability and they also pointed out that vortex pairing events did not occur in their experimental and numerical studies with three-dimensional perturbations. Simoni *et al*. (2014) studied experimentally a transitional separation bubble on a flat plat induced by an adverse gradient typical of ultra-high-lift turbine blade profiles and observed a distinct peak in the spectra, matching the fundamental frequency range. In addition, a subharmonic peak and a higher order harmonic peak are just barely visible in the spectra and they attributed the higher harmonic to the saturation process, and subharmonic to the vortex pairing. A subharmonic peak was also detected in an experimental study on vortex shedding from an airfoil by Yarusevych *et al*. (2009) and they attributed this to the vortex merging. Serna and Lazaro (2014) performed an experimental study of unforced transitional separation bubbles formed on a flat plate due to an adverse pressure gradient at very low turbulence intensity at the test section (< 0.1%). They did not observe the subharmonic mode in the energy spectra and hence they suggested that the pairing mechanism is not active.

All above studies focus on transitional separation bubbles induced by adverse pressure gradients where an attached boundary layer develops before separation, and most of the above studies were carried out under forcing conditions (perturbation at certain frequency and amplitude). Very few studies have been carried out to investigate the secondary instability of a transitional separation bubble where the separation is induced geometrically so that the separation point is fixed at the leading edge and there is no boundary layer developed before the separation point. Abdalla & Yang (2004), and Yang (2013) discussed very briefly secondary instability of a geometrically induced, unforced separation bubble on a flat plate. The focus of this paper is on secondary instability of an unforced transitional separation bubble induced geometrically at the leading edge under a very low free-stream turbulence level (< 0.1%).

2. Flow configuration

The flow configuration in the current study is a flat plate with a blunt leading edge and Figure 1 shows the computational domain and mesh. The size of the computational domain is 25D x 16D x 4D along the x-, y- and z-axis respectively and D is the plate thickness. The width of the computational domain is chosen as 4D, or 0.64 x_R (x_R is the predicted mean separation bubble length of about 6.24D), which is twice the estimated spanwise wavelength of the most amplified secondary instability mode (λ = 0.32 x_R). The Reynolds number based on the uniform inlet velocity and the plate thickness is 6500. The inlet is located at 4.5D upstream of the leading edge of the plate and the outlet is located at x = 20.5D downstream from the leading edge. Both the top and bottom boundaries are at 8D. A grid convergence study in terms of mean flow field was carried out with two meshes, 2.6 and 3.5 million cells with refinement in the wall normal direction only, and the results from the two simulations show little difference, with the maximum discrepancy between the mean streamwise velocity profiles at various locations less than 3%. Hence there is no need to refine the mesh further and the mesh used consists of 256 x 212 x 64 cells (around 3.5 million cells). In terms of wall units based on the friction velocity downstream of reattachment at x/x_R =2.5 the streamwise mesh sizes vary from Δx^+=9.7 to Δx^+=48.5, spanwise mesh is Δz^+=20.2 and the nearest wall mesh size in the vertical direction is Δy^+=2.1. It is crucial to have a good mesh resolution in the transitional flow region to resolve the instability waves and in the present study there are about 50 grid points per streamwise wavelength (mesh is refined in the transitional region) and 32 points per spanwise wavelength.

Random disturbances (white noise) were added to the velocity components at inlet trying to generate a very low free-stream turbulence level of about 0.08% at the plate leading edge. Several test runs with different intensities of the white noise disturbances at inlet were performed to identify that 1.8% was needed to achieve this. The results in terms of the statistical quantities from those runs are the same. At outlet a convective boundary condition is applied. Periodic boundary condition is used in the spanwise direction and a free-slip but impermeable boundary condition is applied on the top and bottom boundaries. On the plate surface a viscous no-slip wall boundary condition is applied without wall functions as the first mesh point is well within the viscous sublayer.

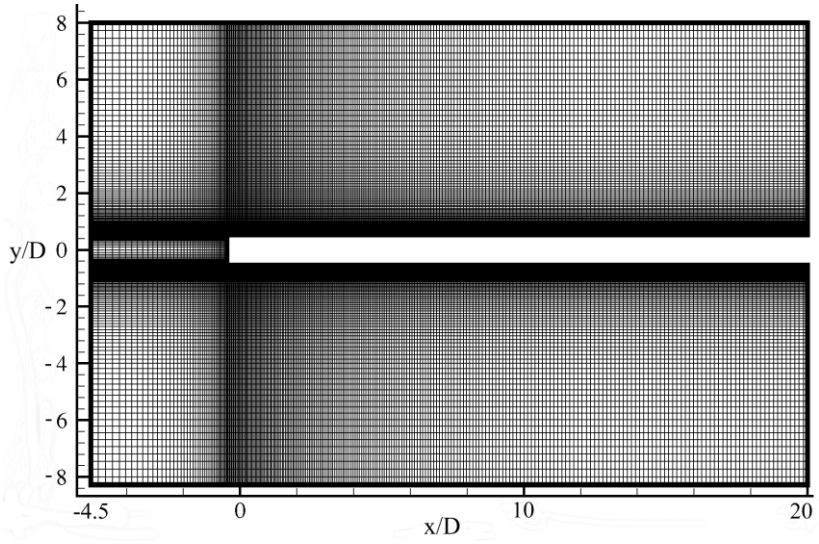

FIG. 1. Computational domain and mesh.

3. Computational details

A well validated in-house LES finite volume code with a staggered grid arrangement is used. The explicit second-order Adams–Bashforth scheme is used for the temporal discretisation and the spatial discretisation is second-order central differencing, which is widely used LES due to its nondissipative and conservative properties. The Poisson equation for pressure is solved by using an efficient hybrid Fourier multigrid method. When the finite volume method is employed the governing equations are integrated over control volumes, equivalent to convolution with a top-hat filter, hence there is no need to apply a filter to the instantaneous equations explicitly and in this case it is called implicit filtering. A dynamic sub-grid-scale model based on Germano *et al*. (1991) and Lilly (1992) is implemented where the model coefficient C is obtained as described in Yang and Voke (2000b, 2001). The mesh is refined in important flow regions where the mesh resolution are quite fine which is not far away from what would be recognized as DNS, with the averaged sub-grid eddy viscosity is below 4 times of the molecular viscosity and the maximum sub-grid eddy viscosity is about 8 times of the molecular viscosity. Therefore the role played by the sub-grid-scale model on the results is very small in the current study. The 2nd order central differencing scheme is used for spatial discretisation. The explicit second order Adams-Bashforth scheme is used for temporal discretisation with a time step of $2x10^{-6}$ second to ensure that the Courant number is below 0.3 for numerical stability. Further details of the mathematical formulation and numerical methods can be found in several papers (Yang and Voke, 2000b, 2001; Abdalla and Yang, 2004, 2005). The simulation ran for 5 flow-through times to allow the flow to become well established and reach a statistically stationary state. The time and spanwise averaged results were gathered over further 28 flow-through times with samples taken every 10 steps.

4. Results and discussion

The LES code used has been very well validated in many transitional studies (Yang and Voke, 2000a, 2001; Abdalla and Yang, 2004, 2005; Yang and Abdalla, 2009) and a comprehensive validation of the predicted mean velocity and Reynolds stresses for the current study can be found in Abdalla and Yang (2004, 2005). The focus here will be on the transition process and especially on the analysis of secondary instability.

4.1. Transition process

The transition process is visualized in Fig. 2, which shows the instantaneous spanwise vorticity at various times (1000-time-step interval) in the (x, y) plane located half way in the spanwise direction (z = 2D). Both the x and y co-ordinates are normalised by the mean separation bubble length x_R. It can be seen that separation occurs at the leading edge and a stable free shear layer develops associated with the formation of two-dimensional spanwise vortices just downstream of the leading edge. The free shear layer develops and is inviscidly unstable a bit further downstream via the Kelvin–Helmholtz mechanism, which has been vigorously demonstrated by Abdalla and Yang (2004). The initial unsteadiness occurs just after x/x_R = 0.2 and this can be confirmed by instantaneous velocity profiles that the position of unsteadiness occurs at about x/x_R = 0.23. It can be seen in Fig.2 that after x/x_R = 0.5, the initial spanwise vortices are distorted severely and roll up, leading to streamwise vorticity formation associated with significant three-dimensional motions, eventually breaking down into relatively smaller turbulent structures after the reattachment point and developing into a turbulent boundary layer rapidly afterward.

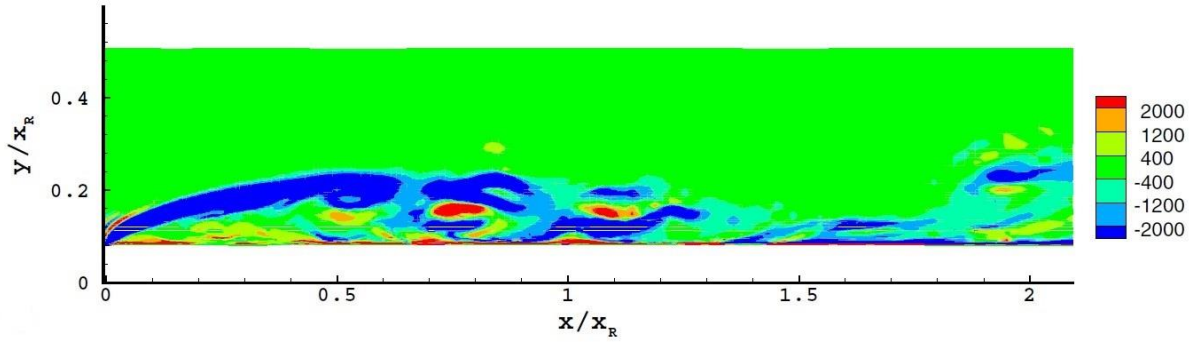

FIG. 2. Instantaneous spanwise vorticity at various times in the (x, y) plane.

4.2. Secondary instability

It was pointed out by Moser and Rogers (1993) that the KH rollers of a plane mixing layer are unstable to two kinds of disturbances: subharmonic disturbances, leading to the pairing of rollers; fundamental three dimensional disturbances, leading to arrays of counter-rotating streamwise vortices called “ribs” which reside in

the braid region between the KH rollers. It was demonstrated by Metcalfe *et al*. (1987) in their study of planar mixing layers that those two secondary instabilities may coexist and compete against each other, and which secondary instability is at work or more dominant depends on flow history such as the initial disturbances, the relative amplitudes of each mode and the external environment in which the flow is embedded etc.

It is evident from several studies that both fundamental mode instability and subharmonic mode instability exist in transitional separation bubbles (McAuliffe and Yaras, 2009; Rist *et al*., 1996; Maucher *et al*., 2000; Marxen *et al*., 2013; Rodriguez and Gennaro, 2015; Jones *et al*., 2008; Simoni *et al*., 2014). Nevertheless in all those studies a separation bubble is formed due to an adverse pressure gradient and in most of those studies some kind of forcing is present to excite certain instability modes. In the present study the separation bubble is formed geometrically at the leading edge without any boundary layer developed before separation and there is no particular kind of forcing to excite any particular instability modes as just random disturbances (white noise) are added to the inlet velocity components to generate a very low free-stream turbulence level. In the following section spectral analysis and flow visualization will be presented to elucidate the secondary instability in the current study.

Pressure correlations have been computed at many locations and there are no obvious peaks appearing in the pressure spectra for locations just after the separation and after the reattachment. Hence only pressure spectra with apparent peaks at locations about half way of the bubble (x/x_R = 0.5) and 75% of the bubble (x/x_R = 0.75) are presented. In addition, it has been found that when streamwise location is fixed the pressure spectra at different spanwise locations are very similar so that all the pressure spectra presented below are at z/l = 0.2.

Figure 3 shows the pressure spectrum at x/x_R = 0.5 and the vertical location is y/x_R = 0.05 (slightly below the centre of the free shear layer, y is measured from the plat surface) and it can be seen that there is only one peak in the spectrum which corresponds to the fundamental frequency (KH instability frequency) but there is no subharmonic peak. Moving vertically upwards along the y axis at the same streamwise location to y/x_R = 0.13 (at the edge of the free shear layer) this fundamental peak becomes more pronounced as shown in Figure 4. There is no sign of subharmonic wave development either. Similarly, only fundamental peak is observed downstream at x/x_R = 0.75 as shown in Figure 5.

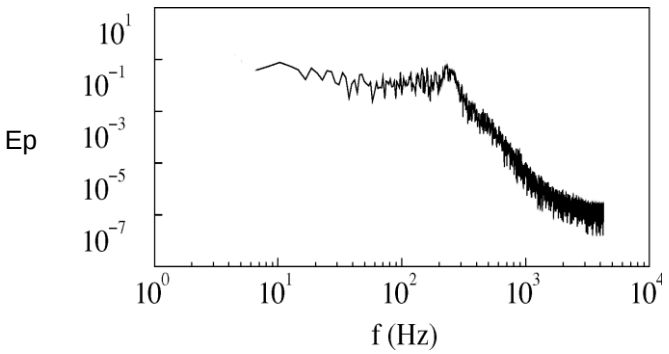

FIG. 3. Pressure spectrum at $x/x_R = 0.5$ and $y/x_R = 0.05$.

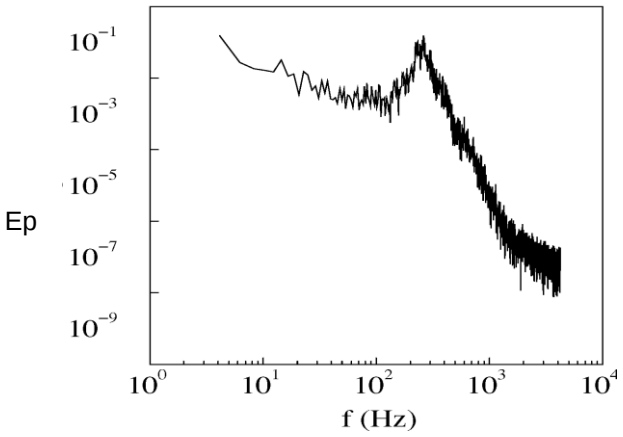

FIG. 4. Pressure spectrum at $x/x_R = 0.5$ and $y/x_R = 0.13$.

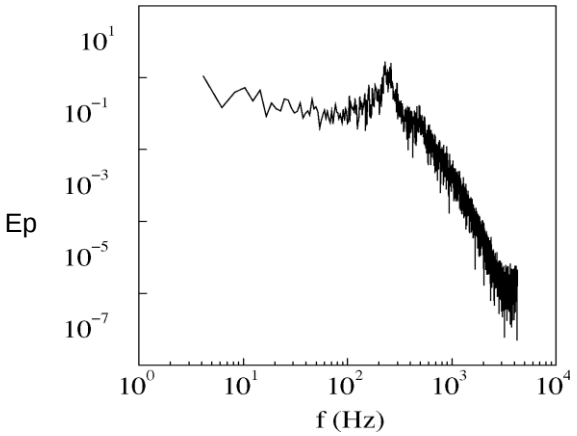

FIG. 5. Pressure spectrum at $x/x_R = 0.75$ and $y/x_R = 0.13$.

Both two dimensional and three dimensional flow visualization have been performed extensively to check the existence of vortex pairing phenomenon initiated by a subharmonic secondary instability. Nevertheless there is no evidence to show the process that two separate spanwise vortices (KH rolls) merge together. It is even very rare to observe two spanwise vortices approaching each other which is captured only once as shown in Figure 6a among the extensive instantaneous data we analysed. It is possible that the structures shown in Figure 6b are due to the vortex pairing but there is no direct evidence to support this speculation, and also this kind of structures are rarely observable among the extensive instantaneous data visualized. Hence in the present study there is no evidence to show the existence of vortex pairing as a result a subharmonic secondary instability form both the spectra analysis and flow visualization.

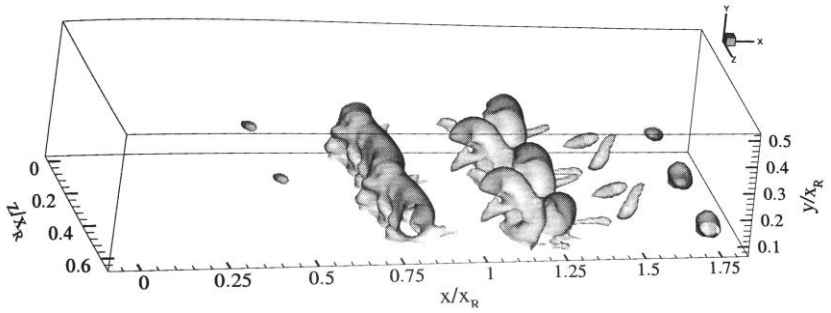

(a)

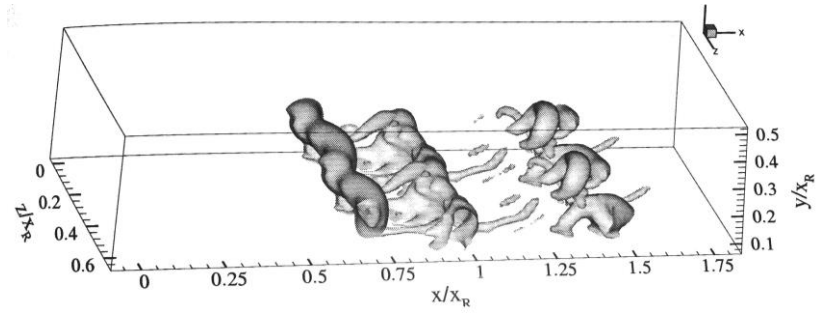

(b)

FIG. 6. Instantaneous pressure iso-surfaces displaying large scale spanwise vortices at different times

Both Marxen *et al.* (2013) and Jones *et al.* (2008) have suggested that two secondary instabilities are likely to be active in transitional separation bubbles: an elliptic instability in the spanwise vortex core region and a hyperbolic instability in the braid region. The elliptic instability is a linear instability mechanism by which three dimensional flows can be generated in regions of two dimensional elliptic streamlines, or can be described as the instability of two dimensional elliptical streamlines to three dimensional disturbances (Kerswell, 2002). The instability mechanism is one of parametric resonance in which a normal mode, or pairs of normal modes, of oscillation on the undistorted circular flow becomes tuned to the underlying strain field. The elliptic instability

will result in a spanwise-periodic deformation of the vortex core and the spanwise wavelength of the most amplified instability mode is about λ = 3d as suggested by Williamson (1996a), where λ is the spanwise wavelength and d is the diameter of the elliptic flow region. Figure 7 shows instantaneous spanwise vortices visualized using pressure iso-surfaces and it can be seen clearly that the first vortex core is deformed periodically in the spanwise direction. It is worked out that in Figure 7a, λ = 2.8d, and λ = 2.6d in Figure 7b, close to the value given by Williamson (1996a).

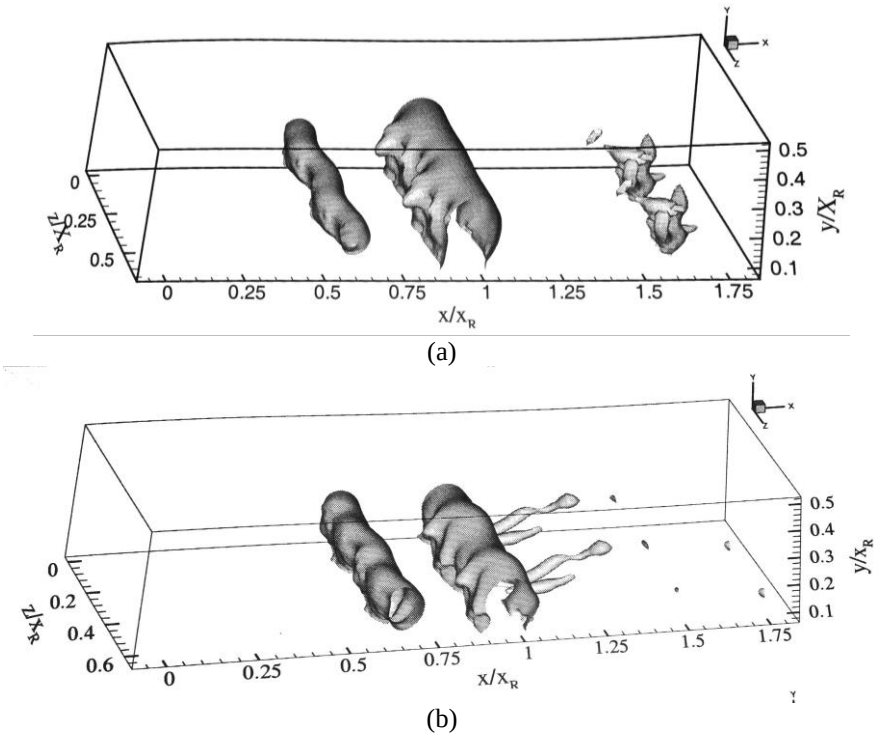

FIG. 7. Instantaneous pressure iso-surfaces at different timings displaying spanwise vortices subject to spanwise waviness

This kind of spanwise periodic waviness has been observed very frequently in the visualization and Figure 8 shows not only the periodically deformed vortex core but also the Λ-shaped vortices resulted from the distorted spanwise KH rolls further downstream. The wavelength in Figure 8a is λ = 2.9d, very close to the elliptical instability wavelength (λ = 3d) given by Williamson (1996a), which strongly indicate that the elliptical instability is active in the present study. Further evidence to support the existence of the elliptical instability in the present study is presented in Figure 9 which shows the velocity vectors and regions of elliptical flow are clearly visible.

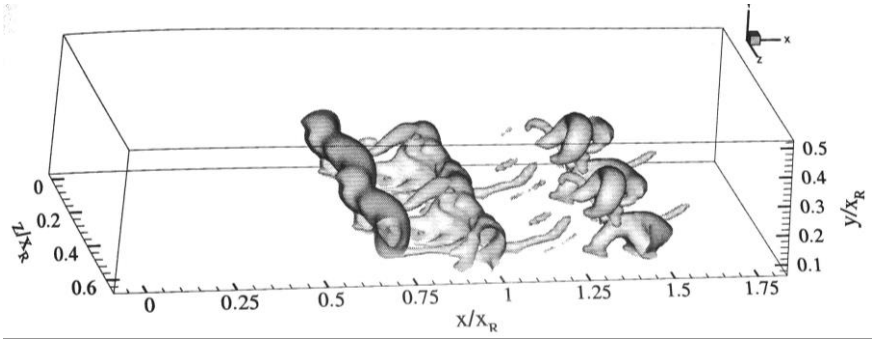

FIG. 8. Pressure iso-surfaces displaying spanwise vortices subject to spanwise waviness and Λ-shaped vortices

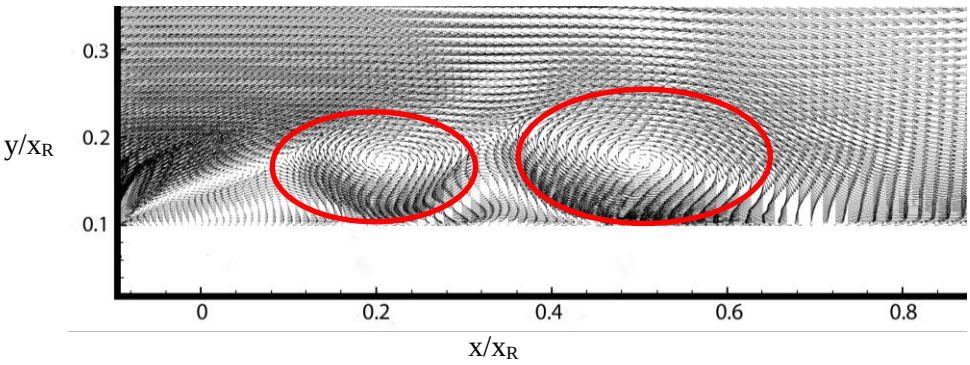

FIG. 9. Velocity vectors showing the region of elliptical flow

Instability in the braid region between spanwise vortices has been observed experimentally in bluff-body wakes (Williamson, 1992, 1996a) and in plane mixing layers (Bernal and Roshko, 1986). Two other studies (Ashurst and Meiburg, 1988; Lasheras and Choi, 1988) have also drawn the conclusion that the streamwise rib vortices are due to a braid-region instability related to the mechanism investigated by Lin and Corcos (1984). It is denoted as hyperbolic instability since it is a manifestation of the instability of two dimensional hyperbolic streamlines in the braid region. The hyperbolic instability leads to the formation of streamwise vortices periodically in the spanwise direction with a wavelength approximately $\lambda = d$ (Williamson, 1996a), much shorter than that in the elliptical instability. Jones *et al.* (2008) observed the presence of hyperbolic flow in the braid region and spanwise periodic streaks of streamwise vortices with a spanwise wavelength roughly $\lambda = d$ in their study of transitional separation bubbles. Therefore they suggested that the hyperbolic instability is active in the braid region. In the study of a transitional separation bubble by Marxen *et al*. (2013) a hyperbolic streamline pattern was also found in the braid region and the ratio of the primary streamwise wavenumber to the spanwsie

wavenumber for one of the mode, mode (1, ±4) in their study, peaking in the braid region is similar to that of the hyperbolic instability behind a circular cylinder (Williamson, 1996b). Hence they suggested that the instability in the braid region is the hyperbolic instability but also pointed out that further evidence was needed to confirm this. Nevertheless several studies in free shear layers suggest that one secondary instability could be responsible for both the deformation of spanwise rollers and the generation of streamwsie 'rib' vortices in the braid region. Pierrehumbert and Widnall (1982) investigated two and three dimensional instabilities of a spatially periodic free shear layer and identified a three dimensional instability which they named it as 'translative instability' as it leads to net translation of spanwise vortex cores rather than bulging. In addition to deforming spanwise rollers the translative instability also leads to array of counter-rotating streamwise 'rib' vortices. They also pointed out that the translative instability is mainly localized in the vortex core region. A study on the three dimensional evolution of a plane mixing layer (Rogers and Moser, 1992) demonstrated that the translative instability responsible for three dimensional growth is not associated with an isolated region of the flow (braid or core region) as it generates continuous growth of both streamwise rib circulation and spanwise roller deformation. In the present study the streamwise rib vortices are clearly visible in the braid region as shown in Figures 8 above and 10 below but there is no other evidence suggesting that the hyperbolic instability is active in the braid region as there are no apparent hyperbolic streamlines observed in the braid region. Furthermore, in Figure 10 the spanwise wavelength of the rib structures is λ = 2.1d and it can be as big as λ = 2.7d as shown in Figure 11, which is quite different from the value associated with the hyperbolic instability λ = d (Williamson, 1996a). Through extensive data analysis in the present study it has been found that the spacing between the streamwise rib vortices varies from λ = 1.9d to λ = 3.1d, which is consistent with the findings by Metcalfe *et al*. (1987) as their results demonstrated the extreme sensitivity of the ribs to the initial or upstream flow conditions, leading to significant variations in the amplitudes and spanwise spacing of the ribs. Substantial scatter was also found in the measurement of the rib spacing by Bernal and Roshko (1986).

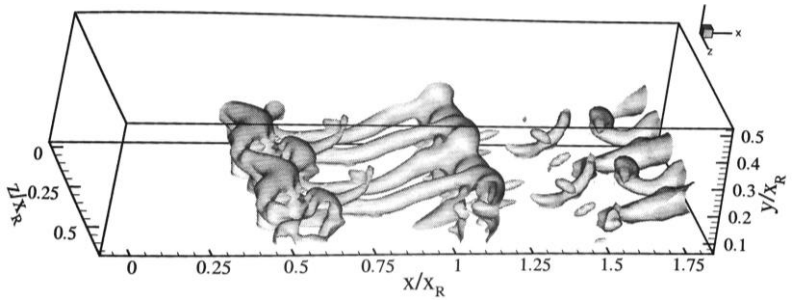

FIG. 10. Pressure iso-surfaces at different timings displaying spanwise vortices and streamwise rib vortices

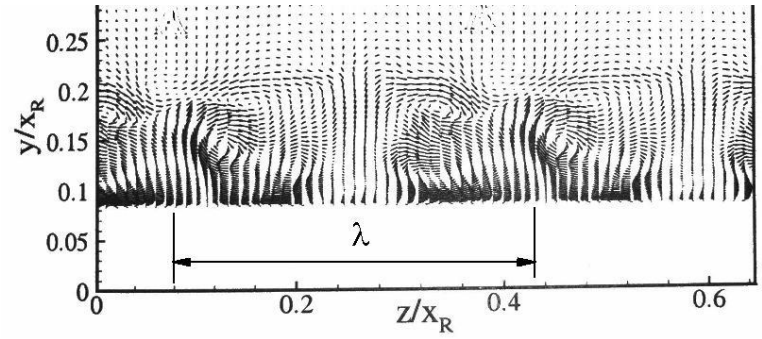

FIG. 11. Velocity vectors in the (y, z) plane showing counter-rotating vortices at $x/x_R = 0.8$.

It is clear from above discussion that there is no general consensus regarding the secondary instabilities at work as some studies suggested the existence of two instabilities, the elliptical instability in the core region leading mainly to the deformation of vortex core and the hyperbolic instability in the braid region leading to the generation of streamwise counter-rotating rib vortices, whereas other studies did not support this idea. In the present study evidence suggests the existence of the elliptical instability but not the hyperbolic instability as the spanwise wavelength of the streamwise ribs varies significantly and very different from the value associated with the hyperbolic instability $\lambda = d$. In fact most of the values of the rib spacing ($2.3d < \lambda < 3.1d$) is actually close to the value associated with the elliptical instability $\lambda = 3d$ and it is possible in the present case that as the elliptical instability progresses part of a deformed spanwise roller lifted up in the free stream, through stretching and titling, counter-rotating streamwise vortices are generated leading to the rib structures as shown in Figures 8 and 10. The evidence presented above suggest that in the present study the secondary instability at work is the elliptical instability which occurs at fundamental frequency only.

It is worth pointing out that instabilities and onset of three dimensionality are very sensitive to variations in initial conditions, forcing and inlet conditions. Variations in amplitude, wavelength, functional form, and relative phasing of the initial low-wavenumber disturbances etc. may excite certain instability modes. In the present study there are no specific disturbances and forcing imposed, and only very low amplitude random disturbances are introduced at inlet to mimic a very low free-stream turbulence level at the leading edge whereas it has been demonstrated that at a higher free-stream turbulence level the primary instability (KH instability) is bypassed (Langari and Yang, 2013), leading to the so called bypass transition where it is very likely that no secondary instability may involve in the transition either.

5. Conclusion

LES study of a transitional separated bubble over a flat plate with a blunt leading edge at a very low free-stream turbulence level (< 0.1%) has been carried out. The separation bubble is induced geometrically at the leading edge. An in-depth analysis has been performed to elucidate the secondary instability active in the transition process.

It is generally accepted that secondary instability can be classified into two main categories: fundamental mode and subharmonic mode, i.e., instability can occur at fundamental and subharmonic frequencies. In the case of a transitional separation bubble and free shear layers the fundamental frequency means the most amplified frequency of disturbances by the two dimensional primary instability, KH instability, and it is also often called free shear layer rollup frequency, KH instability frequency or KH vortex shedding frequency. A subharmonic mode means that an instability occurs at half of the fundamental frequency and it is well established that this is due to pairing of KH rollers. Based on an extensive and in-depth analysis of the power spectra and flow visualization there is no evidence suggesting the existence of vortex pairing phenomenon initiated by a subharmonic secondary instability and the secondary instability is a fundamental mode type in the present study.

Extensive research efforts have been directed at understanding the secondary instability in plane mixing layers and wakes while relatively less efforts have been made towards the secondary instability in transitional separation bubbles. Despite all those efforts there is no general consensus, in fact disagreement as to whether the three dimensional secondary instability is 'a core instability – the elliptical instability', 'a braid instability – the hyperbolic instability', or 'the translative instability' which may be localized in the core region or not associated with an isolated region, or alternatively both core and braid instabilities are present. Evidence in the present study of the transitional separation bubble induced geometrically over a flat plate with a blunt leading edge without any particular kind of forcing suggests that the only secondary instability at work is the elliptical instability, which occurs at fundamental frequency and responsible for both the KH roller deformation and the formation of streamwsie rib vortices.

Funding: This research did not receive any specific grant from funding agencies in the public, commercial, or not-for-profit sectors.

References

Abdalla, I.E., Yang, Z., 2004. Numerical study of the instability mechanism in transitional separating-reattaching flow. Int. J. Heat and Fluid Flow 25, 593-605. http://doi.org/10.1016/j.ijheatfluidflow.2004.01.004.

Abdalla, I.E., Yang, Z., 2005. Numerical study of a separated–reattached flow on a blunt plate. AIAA Journal 43, 2465-2474. http://dx.doi.org/10.2514/1.1317.

Ashurst, W.T., Meiburg, E., 1988. Three-dimensional shear layers via vortex dynamics. J. Fluid Mech. 189, 87-116. DOI: https://doi.org/10.1017/S0022112088000928.

Bernal, L.P., Roshko, A., 1986. Streamwise vortex structure in plane mixing layers. J. Fluid Mech. 170, 499-525. DOI: https://doi.org/10.1017/S002211208600099X.

Burgmann, S., Dannemann, J., Schroder, W., 2008. Time-resolved and volumetric PIV measurements of a transitional separation bubble on an SD7003 airfoil. Experiments in Fluids 44, 609-622. DOI: 10.1007/s00348-007-0421-0.

Dahnert, J., Lyko, C., Peitsch, D., 2012. Transition mechanisms in laminar separated flow under simulated low pressure turbine aerofoil conditions. Journal of Turbomachinery 135, 011007. DOI: 10.1115/1.4006393.

Germano, M., Piomelli, M., Moin, P., Cabot, W.H., 1991. A dynamic subgrid-scale eddy viscosity model. Physics of Fluids A 3, 1760-1765. DOI: http://dx.doi.org/10.1063/1.857955.

Herbert, T., 1988. Secondary instability of boundary layers. Annu. Rev. Fluid Mech. 20, 487-526. DOI: 10.1146/annurev.fl.20.010188.002415.

Ho, C.M., Huerre, P., 1984. Perturbed free shear layers. Annu. Rev. Fluid Mech. 16, 365-422. DOI: 10.1146/annurev.fl.16.010184.002053.

Huang, L.S., Ho, C.M., 1990. Small-scale transition in a plane mixing layer. J. Fluid Mech. 210, 475-500. DOI: https://doi.org/10.1017/S0022112090001379.

Istvan, M.S., Yarusevych, S., 2018. Effects of free-stream turbulence intensity on transition in a laminar separation bubble formed over an airfoil. Experiments in Fluids 59, 52:1-21. https://doi.org/10.1007/s00348-018-2511-6.

Jones, L.E., Sandberg, R., Sandham, N.D., 2008. Direct numerical simulations of forced and unforced separation bubbles on an airfoil at incidence. J. Fluid Mech. 602, 175-207. DOI: https://doi.org/10.1017/S0022112008000864.

Kerswell, R.R., 2002. Elliptical instability. Annu. Rev. Fluid Mech. 34, 83-113. DOI: 10.1146/annurev.fluid.34.081701.171829.

Lasheras, J.C., Choi, H., 1988. Three-dimensional instability of a plane free shear layer: an experimental study of the formation and evolution of streamwise vortices. J. Fluid Mech. 189, 53-86. DOI: https://doi.org/10.1017/S0022112088000916.

Langari, M., Yang, Z., 2013. Numerical study of the primary instability in a separated boundary layer transition under elevated free-stream turbulence. Phys. Fluids 25, 074106-1-12. http://dx.doi.org/10.1063/1.4816291.

Lilly, D.K., 1992. A proposed modification of the Germano subgrid-scale closure method. Physics of Fluids A 4, 633-635. DOI: http://dx.doi.org/10.1063/1.858280.

Lin, S.J., Corcos, G.M., 1984. The mixing layer: deterministic models of a turbulent flow. Part 3. The effect of plane strain on the dynamics of streamwise vortices. J. Fluid Mech. 141, 139-178. DOI: https://doi.org/10.1017/S0022112084000781.

Manneville, P., 1990. Dissipative Structures and Weak Turbulence, Academic Press, San Diego.

Marxen, O., Lang, M., Rist, U., Wagner, S., 2003. A combined experimental/numerical study of unsteady phenomena in a laminar separation bubble. Flow Turbul. Combust. 71, 133-146. doi:10.1023/B:APPL.0000014928.69394.50.

Marxen, O, Lang, M., Rist, U., 2013. Vortex formation and breakup in a laminar separation bubble. J. Fluid Mech. 728, 58-90. DOI: https://doi.org/10.1017/jfm.2013.222.

Maucher, U., Rist, U., Wagner, S., 1999. Transitional structures in a laminar separation bubble. In: Nitsche, W., Heinemann, H., Hilbig, R. (Eds), New Results in Numerical and Experimental Fluid Mechanics II. Vieweg, pp. 307–314.

Maucher, U. Rist, U., Wagner, S., 2000. Secondary disturbance amplification and transition in laminar separation bubbles. In: Fasel, H., Saric, W. (Eds), Laminar-Turbulent Transition. Springer, Berlin, pp. 657–662. DOI: 10.1007/978-3-662-03997-7_102.

McAuliffe, B.R., Yaras, M.I., 2009. Passive manipulation of separation-bubble transition using surface modifications. J. Fluids Engineering 131, 021201. doi:10.1115/1.2978997.

McAuliffe, B.R., Yaras, M.I., 2010. Transition mechanisms in separation bubbles under low- and elevated-freestream turbulence. Journal of Turbomachinery 132, 011004. doi:10.1115/1.2812949.

Metcalfe, R.W., Orszag, S.A., Brachet, M.E., Menon, S., Riley, J.J., 1987. Secondary instability of a temporally growing mixing layer. J. Fluid Mech. 184, 207-243. DOI: https://doi.org/10.1017/S0022112087002866.

Michelis, T., Yarusevych, S., Kotsonis, M., 2018. On the origin of spanwise vortex deformations in laminar separation bubbles, J. Fluid Mech. 841, 81-108. DOI: 10.1017/jfm.2018.91.

Moser, R.D., Rogers, M.M., 1993. The three-dimensional evolution of a plane mixing layer: pairing and transition to turbulence. J. Fluid Mech. 247, 275-320. DOI: https://doi.org/10.1017/S0022112093000473.

Pierrehumbert, R.T., Widnall, S.E., 1982. The two- and three-dimensional instabilities of a spatially periodic shear layer. J. Fluid Mech. 114, 59-82. DOI: https://doi.org/10.1017/S0022112082000044.

Rist, U., Maucher, U., Wagner, S., 1996. Direct numerical simulation of some fundamental problems related to transition in laminar separation bubbles. In: Computational Methods in Applied Sciences ’96, ECCOMAS. John Wiley & Sons Ltd., pp. 319-325.

Rodrıguez, D., Gennaro, E.M., 2015. On the secondary instability of forced and unforced laminar separation bubbles. Procedia IUTAM 14, 78-87. https://doi.org/10.1016/j.piutam.2015.03.026.

Rogers, M.M., Moser, R.D., 1992. Three-dimensional evolution of a plane mixing layer: the Kelvin-Helmholtz rollup. J. Fluid Mech. 243, 183-226. DOI: https://doi.org/10.1017/S0022112092002696.

Sarkar, S., 2008. Identification of flow structures on a LP turbine blade due to periodic passing wakes. J Fluid Eng. 130, 061103. DOI:10.1115/1.2911682

Satta, F., Simoni, D., Ubaldi, M., Zunino, P., Bertini, F., 2010. Experimental investigation of separation and transition processes on a high- lift low-pressure turbine profile under steady and unsteady inflow at low Reynolds number. Journal of Thermal Science 19, 26-33. DOI: 10.1007/s11630-010-0026-4.

Schmid P.J., Henningson, D.H., 2001. Stability and Transition in Shear Flows, Springer, New York.

Seran, J., Lazaro, B.J., 2014. The final stages of transition and the reattachment region in transitional separation bubbles. Experiments in Fluids 55, 1695-1-17. DOI: 10.1007/s00348-014-1695-7.

Simoni, D., Ubaldi, M., Zunino, P., 2014. Experimental investigation of flow instabilities in a laminar separation bubble. Journal of Thermal Science 23, 203-214. DOI: 10.1007/s11630-014-0697-3.

Simoni, D., Lengani, D., Ubaldi, M., Zunino, P., Dellacasagrande, M., 2017. Inspection of the dynamic properties of laminar separation bubbles: free-stream turbulence intensity effects for different Reynolds numbers. Experiments in Fluids 58, 66:1-14. https://doi.org/10.1007/s00348-017-2353-7.

Williamson, C.H.K., 1992. The natural and forced formation of spot-like 'vortex dislocations' in the transition of a wake. J. Fluid Mech. 243, 393-441. DOI: https://doi.org/10.1017/S0022112092002763.

Williamson, C.H.K, 1996a. Three-dimensional wake transition. J. Fluid Mech. 328, 345-407. DOI: https://doi.org/10.1017/S0022112096008750.

Williamson, C.H.K., 1996b. Vortex dynamics in the cylinder wake. Annu. Rev. Fluid Mech. 28, 477-539. DOI: 10.1146/annurev.fl.28.010196.002401.

Yang, Z., Voke, P.R., 2000a. On early stage instability of separated boundary layer transition. In: Dopazo, C. (Ed), Advances in Turbulence VIII. CIMNE, Spain, pp. 145-148.

Yang, Z., Voke, P.R., 2000b. Large-eddy simulation of separated leading-edge flow in general co-ordinates. Int. J for Num. Meth. In Engineering 49, 681-696. DOI: 10.1002/1097-0207(20001020)49:5<681::AID-NME975>3.0.CO;2-F.

Yang, Z., Voke, P.R., 2001. Large-eddy simulation of boundary layer separation and transition at a change of surface curvature. J. Fluid Mech. 439, 305-333. DOI: https://doi.org/10.1017/S0022112001004633.

Yang. Z, Abdalla, I.E., 2009. Effects of free-stream turbulence on a transitional separated–reattached flow over a flat plate with a sharp leading edge. Int. J. Heat and Fluid Flow 30, 1026-1035. http://doi.org/10.1016/j.ijheatfluidflow.2009.04.010.

Yang, Z., 2013. Numerical study of instabilities in separated-reattached flows. Int. J. Comp. Meth. and Exp. Meas. 1, 116-131. DOI: 10.2495/CMEM-V1-N2-116-131.

Yarusevych, R., Sullivan, P., Kawall, J.G., 2009. On vortex shedding from an airfoil in low-Reynolds-number flows. J. Fluid Mech. 632, 245-271. DOI: https://doi.org/10.1017/S0022112009007058.